Article

# Nyrdvomenshor Gem Stones Deposit, Polar Urals, Russia

Evgeniy V. Kislov * , Mikhail P. Popov , Firat M. Nurmukhametov , Viktor F. Posokhov , Vladislav V. Vanteev

Posted Date: 17 April 2023

doi: 10.20944/preprints202304.0434.v1

Keywords: nephrite; diopsidite; rodingite Nyrdvomenshor; uvarovite; chromite; metamorphism; metasomatism

*Preprints* (www.preprints.org) | NOT PEER-REVIEWED | Posted: 17 April 2023 doi:10.20944/preprints202304.0434.v1

*Article*

# Nyrdvomenshor Gem Stones Deposit, Polar Urals, Russia

**Evgeniy V. Kislov [1,2,*], Mikhail P. Popov [2,3], Firat M. Nurmukhametov [3], Viktor F. Posokhov [1] and Vladislav V. Vanteev [1]**

[1] Dobretsov Geological Institute, Siberian Branch of the Russian Academy of Sciences, 670047 Ulan-Ude, Russia; evg-kislov@ya.ru
[2] Zavaritsky Institute of Geology and Geochemistry of the Ural Branch of the Russian Academy of Sciences, 620016, Ekaterinburg, Russia; popovm1@yandex.ru
[3] Ural State Mining University, 620014, Ekaterinburg, Russia
* Correspondence: evg-kislov@ya.ru

**Abstract:** We have studied quality characteristics, chemical, mineral and isotope composition of nephrite, diopsidite and rodingite of the Nyrdvomenshor deposit in the Polar Urals. We applied the visual petrographic and mineralogical studies, X-ray spectral fluorescence, ICP-MS analysis, scanning electron microscope with the dispersive microanalysis system, oxygen isotope composition was measured. According to its quality characteristics, the nephrite is substandard. Here, uvarovite, which forms idiomorphic grains, sometimes sheath-like, less often xenomorphic elongated, and substituting chromite are commonly encountered. The nephrite was formed due to both metamorphic and metasomatic processes. Serpentinite was replaced by diopsidite, which was then replaced by nephrite. Metamorphism intensified metasomatism of the serpentinite melange and provided a cryptocrystalline tangled-fibrous structure of the nephrite. Then metamorphism and metasomatism led to the formation of omphacite and cracking of the nephrite, which reduced its quality. As these processes progressed, contribution of crustal fluid increased.

**Keywords:** nephrite; diopsidite; rodingite Nyrdvomenshor; uvarovite; chromite; metamorphism; metasomatism

## 1. Introduction

Nephrite consist of fibrous tremolite mainly. It is a highly valuable jewelry and ornamental stone, long used by humankind, especially popular in China, New Zealand, and Central America. The most expensive units are white translucent, black, bright green with a minimum amount of ore minerals, with the "cat's eye" effect nephrites, alluvial pebbles with edges of coloring.

Nephrite deposits belong to two endogenous geological industrial types: after ultramafic metasomatites of ophiolites (serpentinite type, S type) and after carbonate tremolite-calcite magnesian skarns (dolomite type, D type) [1,2]. The Dahua deposit in the Guangxi Zhuang Autonomous Region [3] and Luodian deposit in Guizhou Province [4] in southern China, formed on the contact of diabases and limestones, are close to the D type. Deposits of the S type are a source of predominantly green to brown and black nephrite, deposits of the D type produce mainly light-colored nephrite from white to light green, brown (honey) due to oxidation of divalent iron to trivalent, black nephrite is less common [3,5]. The exogenous geological industrial type is represented by placers, of which alluvial ones are the most productive.

In China, D type nephrite deposits are most common, so they are best studied. There are few deposits of S type nephrite outside of Russia. In China, the Manas deposit in the Northern Tien Shan in the Xinjiang Uygur Autonomous Region is practically worked out [6,7]. Nephrite of both S type and D type is mined from the famous Golmud deposit in the central part of Qinghai province [8]. The Yushigou (Qilian) S-type nephrite deposit is mined in the north of Qinghai Province [9]. The Shimian deposit in Sichuan Province is famous for producing high-quality nephrite with chatoyancy [10,11]. The Fengtien deposit is known in Taiwan [12–14]. Recently, nephrite from the border areas of

Pakistan and Afghanistan has appeared on the market [15–18]. The Shaitantas deposit in the Karaganda region of Kazakhstan [19], Co Phuong deposit in Shonla Province in Vietnam have been poorly studied.

A number of S-type nephrite deposits are located on the Pacific coast of North America from Guatemala to Alaska, mining are carried out mainly at British Columbia in Canada [20–23]. Deposits are known, but poorly studied in Wyoming, USA [24]. Deposits Jordanov and Nasławice in Poland were mainly worked out in the XIX century, when they were located on the territory of Prussia under the names Jordansmühl and Naselwitz [24–26]. There are small deposits that have been worked out in Austria and Switzerland. Small S-type nephrite deposits have long been known on the South Island of New Zealand [24,27–29] and in New South Wales in Australia [30,31].

As of January 1, 2022, the Russian State reserve balance includes 26 nephrite deposits. 7 deposits are developed in Buryatia Republic, including the serpentinite type nephrite deposits Khamarkhuda in the Khamar-Daban and Ospa (22.99% of reserves and 47.64% of Russian production) in the Eastern Sayans. Deposits of the serpentinite type Kurtushiba (Eastern Section) in the Western Sayans, Tuva Republic, also Onot, Arakhushanzhalga, Pole Tchudes (Field of Miracles), Ulan-Khoda, Khusha-Gol, Gorlykgol (25.15 and 6.95%) in the Eastern Sayans, Buryatia are prepared for development. The deposits Kantegir, Kurtushiba (Central Section), Stan-Taskyl in the Western Sayans, Krasnoyarsk region and Sagan-Sayr in the Eastern Sayans, Buryatia are explored. The unallocated mineral resources fund (not transferred to development) includes the Academia deposit in the Southern Urals, Chelyabinsk region, Boldokit and Zun-Ospa in the Eastern Sayans, Khangarul and Kharganta in the Khamar-Daban, Buryatia. Many manifestations that are not put on the State Balance sheet are also explored.

A number of little deposits of S-type nephrite is known in the Urals. The first single finds were made in the area of the Muldakaev place [32] and on Mount Bikilar [33] in the area of Miass at South Urals. The Nyrdvomenshor deposit is known in the Polar Urals [19,34]. In the Middle Urals, nephrite was found in the alluvium of the Neivo-Rudyanka near the Pyshma town [35] and the Bazhenov chrysotile asbestos deposit [36].

There are three nephrite places in Bashkir republic: Kozma-Demyan near the talc deposit of the same name in the north-east of Bashkiria – nephrite blocks on the banks of the Maly Iremel River; in the south-east of Bashkiria, Keusht – primary outlets with an area of 1.5-2 $m^2$; Kildigul on the right side of the valley of the Saraga River – a primary outlet, 10×5 m in size, in the polymict serpentinite melange of the Kraka complex [37]. The Khalil nephrite deposit was discovered in 1968 in the Khalil ultramafic massif at the Orenburg region [19]. On the southern extension of the Urals, there is the Dzhetygara place of nephrite in Kazakhstan [38].

In 2003, the Akademia deposit with Student and Facultet sites was discovered in the vicinity of Miass in the Chelyabinsk region [39]. There is the Uchaly-Miass potentially nephrite-bearing area traced from north to south from the city of Karabash through Miass to the city of Uchaly [40]. Nevertheless, in the Urals, nephrite was mined in a limited volume at the Nyrdvomenshor and Academia deposits. At present, mining is not performed here.

Despite the significant number of deposits and manifestations of after serpentinite nephrite, their geology and genesis is not sufficiently studied. The idea of metasomatic origin of the nephrite is the most popular [1,2], some authors hold the opinion about the predominant role of metamorphism [41]. This study is aimed at studying the material composition of the nephrite at the Nyrdvomenshor deposit in order to clarify the features of its origin.

## 2. Materials and Methods

In order to assess the quality and composition of the nephrite from the Nyrdvomenshor deposit, which includes the Nyrdvomenshor and Ray-Iz sites, we have studied 8 polished plates of alluvial material. An angular rodingite sample and a polished jadeite plate were examined as additional material.

Visual petrographic and mineralogical studies were performed in natural light, using photofixation. Decorative properties (color, shade, pattern, presence of edges, degree of roughness) were determined using a MBS-10 binocular microscope and a special flashlight CYZ-B05.

The chemical composition of the rocks was determined by the X-ray spectral fluorescence method on an XRF-1800 wave X-ray fluorescence spectrometer (SHIMADZU, Japan) at the "Geoanalitic" Research Center at IGG UrB RAS, Ekaterinburg according to the method [42], analysts N.P. Gorbunova, L.A. Tatarinova, I.A. Zhelunitsyn, A.A. Nekrasova.

The samples were decomposed and the impurity element content was analyzed using ICP-MS analysis at the "Geoanalitic" Research Center at IGG UrB RAS, analyst D.V. Kiseleva on a NexION300S quadrupole ICP mass spectrometer, Perkin Elmer, USA. The microwave decomposition of the samples was carried out by a mixture of HCl + $HNO_3$ + HF acids using the Berghof Speedwave MWS 3+ system. Typical operating conditions of the mass spectrometer are as follows: power of the radio frequency generator is 1300 W, material of the interface cones is platinum. All measurements were carried out on the mode of quantitative analysis with the construction of calibration curves. Multi-element standard solutions certified in accordance with ISO 9001 Perkin Elmer Instruments were used to construct the calibration dependencies. Certified samples of BCR-2 basalt and AGV-2 andesite USGS were used to control the correctness and accuracy while determining the trace element composition. The obtained concentrations of rare, scattered and rare-earth elements correspond to the certified values with an acceptable deviation within 15%. The errors in element identification are (rel. %): 24 (Cr, Ni, Co, Cu, V, Ba, Sr), 30 (Rb), 41 (РЗЭ), 50 (Zr), 60 (Y, Hf, Ta, Nb, Th, U).

The mineral composition was studied using a LEO-1430VP scanning electron microscope, Carl Zeiss, Germany, with the INCA Energy 350 energy dispersive microanalysis system, Oxford Instruments, UK, at the "Geospectr" Research Center at GIN SB RAS, Ulan-Ude, analyst E.A. Khromova. The research conditions are as follows: accelerating voltage - 20 kV, probe current - 0.3-0.4 nA, probe size - <0.1 microns, measurement time - 50 seconds (live time), the analysis error in the amount reaches 2-4 wt. % depending on the quality of the sample surface and the characteristics of its composition. The content of trivalent iron was calculated by stoichiometry.

The oxygen isotope composition was measured on a FINNIGAN MAT 253 gas mass spectrometer at the "Geospectr" Research Center at GIN SB RAS, Ulan-Ude, analyst V.F. Posokhov, using the double intake system in the classical version, standard sample. To determine $^{\delta 18}O$ values, the samples were prepared using the laser fluorination (LF) method on the mode "laser ablation with oxygen extraction from silicates" in the presence of $BrF_5$ reagent according to the method [43]. The calculations were made with respect to the $O_2$ working standard, calibrated at the V-SMOW scale by regular oxygen measurements in the international standards NBS-28 quartz and NBS-30 biotite. The correctness of the values obtained was controlled by regular measurements of its own internal standard GI-1 quartz and laboratory IGEM RAS Polaris quartz. The measurement error of the obtained $\delta^{18}O$ values was at the level of (1s) ± 0.2 %.

## 3. Results

### *3.1. Geology of Nyrdvomenshor deposit*

The Nyrdvomenshor deposit is located on the contact of the Rai-Iz ultramafite massif in the Polar Urals in the basin of the upper and middle reaches of the Nyrdvomenshor stream, 56 km northwest of Labytnangi tawn in the Priuralsky district of the Yamalo-Nenets Autonomous Okrug.

Nephrite was found here in 1974 by "Sevkvartssamotsvety" enterprise. In 1975-1980, 250 nephrite and 60 jadeite locations were found in the bedrock and boulder placers. Some of them were industrially assessed and underwent pilot testing with inventory calculation. In 1980-1981, 21.8 tons of ornamental nephrite (1st grade) were mined from alluvial placers. Protocol № 20\7 of 26 February 1982 by the Ministry of Geology of the USSR approved the nephrite reserves 21.8 tons. In 1985-1990, the Polar-Ural Geological Exploration Expedition performed 1:50000 survey of this area. In 1991, the "Nord Rifei" enterprise reassessed the nephrite and jadeite sites. Protocol No. 46\91 of 28 December

doi:10.20944/preprints202304.0434.v1

1991 by "Zapsibkomgeologiya" geological section tested the forecast resources: nephrite – 1 000 tons; jadeite – 5000 tons, jasper – 10 000 tons.

On the 14th of October 2013, the Department for Subsoil Use in the Yamalo-Nenets Autonomous Okrug put up the Nyrdvomenshor site (nephrite, jadeite, jasper) for auction. 4 companies submitted an application, but were not admitted to the auction, the auction did not happen. On the 31st of July 2014, the authorities of the Yamalo-Nenets Autonomous Okrug established the Polar-Urals Nature Park, which included the territory of the licensed area. By According to protocols No. 24-TV of 25 December 2019 and No. 12-TV of 6 October 2020, "NTS-Uralnedra" tested the forecast resources of nephrite, jadeite and jasper of the Rai-Iz, which was not included in the natural park: nephrite (raw) – 3 000 tons; jadeite (raw) – 15 000 tons; jasper (raw) – 11 000 tons. On the 9th of November 2020, the Department for Mineral Resources in the Ural Federal District announced an auction for the right to use the subsoil for the purpose of geological study, exploration and extraction of nephrite, jadeite and jasper at the Rai Iz site. According to the results of the auction, the license was issued to "Salekhard Mining Enterprise".

The deposit is confined to the zone of northern tectonic contact along the Main Ural fault of the Ray-Iz ultramafic massif with metamorphic and intrusive rocks of the Harbey block of the Middle-Late Proterozoic and metamorphosed sedimentary-volcanogenic rocks of the Lemvin structural-facies zone of Paleozoic age (Figure 1). The Rai-Iz massif is composed mainly of harzburgites, dunites and serpentinites, formed after them [44]. Paleozoic sedimentary-volcanogenic formations are represented by clay-siliceous and carbonaceous-siliceous shales with interlayers of metaeffusives of ultramafic composition. The contact of the Rai-Iz massif along the Main Ural fault is a zone of polymictic melange with formations of diopsidites, rodingites, plagioclasites, albite-jadeites, nephrites. Eluvial-deluvial, fluvioglacial and alluvial deposits are common.

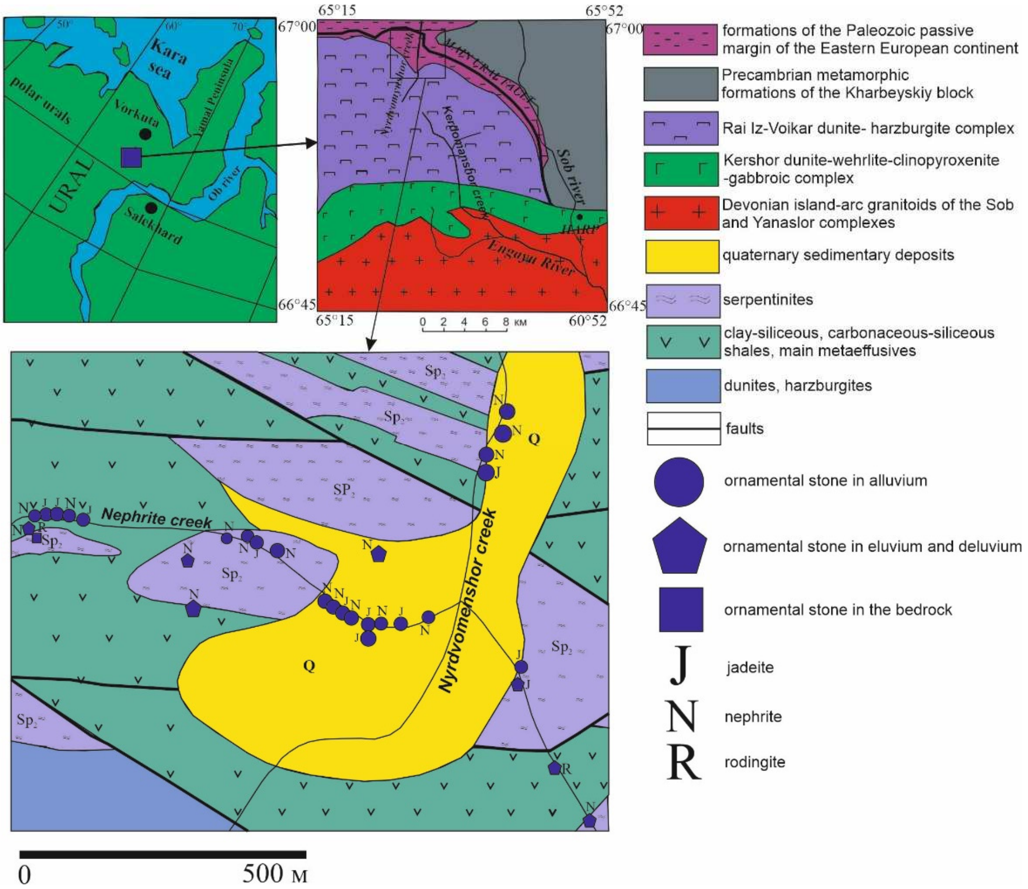

**Figure 1.** Scheme of the Nyrdvomenshor deposit. The right inset shows the eastern part of the Rai-Iz massif according to [45].

doi:10.20944/preprints202304.0434.v1

1 – formations of the Paleozoic passive margin of the Eastern European continent; 2 – Precambrian metamorphic formations of the Kharbeyskiy block; 3 1 – Rai Iz-Voikar dunite-harzburgite complex; 4 – Kershor dunite-wehrlite-clinopyroxenite-gabbroic complex; 5 – Devonian island-arc granitoids of the Sob and Yanaslor complexes; 6 – quaternary sedimentary deposits; 7 – serpentinites; 8 – clay-siliceous, carbonaceous-siliceous shales, main metaeffusives; 9 – dunites, harzburgites; 10 – faults; 11 – ornamental stone in alluvium; 12 - ornamental stone in eluvium and deluvium; 13 – ornamental stone in the bedrock; 14 – jadeite; 15 – nephrite; 16 – rodingite.

Nephrite sites are known to be in bedrocks, piles and placers, mostly in the area of the Nyrdvomenshor and Kharamatalaus faults (Figure 2) within serpentine melange (Figure 3), in the contact zones of after gabbro bodies. In the bedrock, nephrite forms more than 300 lenticular veins with a length of 1-60 m, and a thickness of several centimeters to 3 m. There are five main types of nephrite localization: veins in serpentinites; on the contact of serpentinites and metaeffusives; metaeffusives; on the contact of after gabbroid rodingites and serpentinites; in rodingites [19].

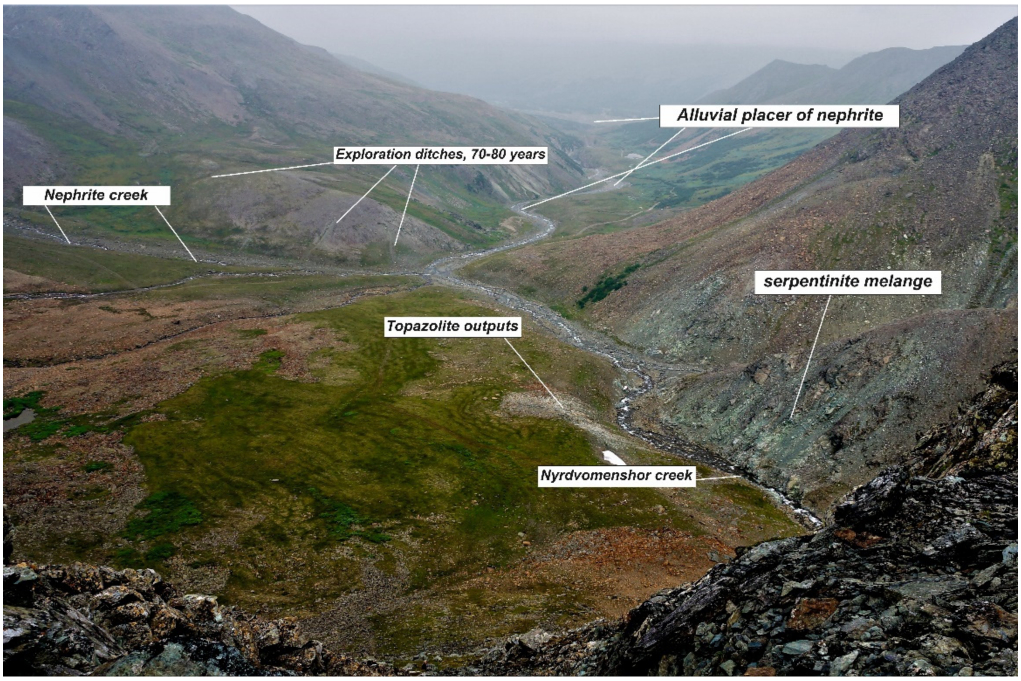

**Figure 2.** Photo of the Nyrdvomenshor deposit.

The erosion of most nephrite veins provided the bulk of block-boulder material that makes up the industrial glacial-alluvial placer deposit – the main object of nephrite extraction (Figure 4). During the boulder transportation, there was a natural improvement in the quality of nephrite due to abrasion of the talc-tremolite sheath [19]. The alluvial placer of nephrite is confined to the channel and floodplain parts of the Nyrdvomenshor Creek and its tributaries – the Nephritovyi and Obraztsovyi streams. The width of the placer ranges from 20-60 m, the length is up to 4.5 km. The size of the nephrite boulders is 0.1-2.9 m. The average frequency of occurrence is 1 boulder per 680-700 m$^2$.

**Figure 3.** Block of nephrite in serpentinite melange.

**Figure 4.** Alluvial block of nephrite.

### *3.1. Diopside and rodingite*

Two samples 162 and 3/12 (Figure 5) are represented by diopsidites, “karkaro” [1]. No. 162 is grayish-white with greenish streaks of uvarovite and black grains of chromite, no. 3/21 is of heterogeneous light green color due to uneven distribution of tremolite and chlorite.

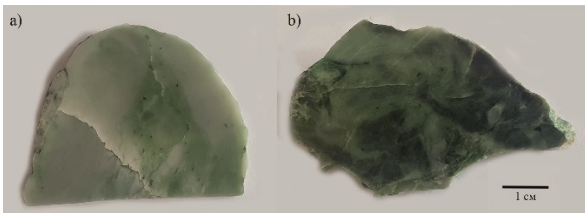

**Figure 5.** Diopsidite samples: a) – 162; b) – 3/21.

Fine-grained diopside (Table 1) prevail in the composition of diopsidite; cloud-like aggregates of chlorite, streaks of chlorite with grains of chromite and uvarovite (one analysis corresponds to andradite), small idiomorphic and xenomorphic grains of heazlewudite (in 6 grains of sample 162, Ni – 71.46-74.23%, S – 25.75-27.72%, in 3 grains of sample 3/31, Fe – 0.67-2.22%, Ni – 62.90-71.77%, S – 26.20-33.25%) are characteristic. Chromite grains are split by chlorite veins. Uvarovite corrodes and overgrows chromite. Tremolite, pentlandite with an admixture of cobalt, stibnite with an admixture of iron intergrown with heazlewudite, titanite with an inclusion of ilmenite in a small amount appear in sample 3/21, and tremolite makes cracks in chromite.

**Table 1.** Chemical composition of diopsidites minerals, wt. %.

| | $SiO_2$ | $TiO_2$ | $Al_2O_3$ | $Cr_2O_3$ | FeO | $Fe_2O_3$ | MnO | MgO | CaO | $Na_2O$ | NiO | ZnO | $V_2O_3$ | ∑ |
|---|---|---|---|---|---|---|---|---|---|---|---|---|---|---|
| | | | | | | diopside (14) | | | | | | | | |
| Min | 52.86 | 0 | 0 | 0 | 2.38 | 0 | 0 | 11.67 | 20.85 | 0 | 0 | 0 | 0 | 98.29 |
| Max | 57.44 | 0.35 | 1.70 | 0.63 | 12.43 | 0.10 | 0.58 | 17.96 | 24.95 | 1.04 | 0 | 0 | 0 | 101.95 |
| | | | | | | garnet (11) | | | | | | | | |
| Min | 35.62 | 0.90 | 0 | 6.23 | 0.90 | 0 | 0 | 0 | 29.58 | 0 | 0 | 0 | 0 | 98.07 |
| Max | 37.91 | 3.12 | 10.68 | 19.83 | 4.35 | 20.27 | 0.58 | 3.42 | 34.08 | 0 | 0 | 0 | 0 | 101.45 |
| | | | | | | tremolite (4) | | | | | | | | |
| Min | 55.49 | 0 | 0 | 0 | 4.05 | - | 0 | 11.92 | 12.41 | 0 | 0 | 0 | 0 | 95.43 |
| Max | 58.85 | 0.38 | 3.95 | 0 | 4.43 | - | 0.56 | 22.07 | 18.19 | 3.79 | 0 | 0 | 0 | 98.82 |
| | | | | | | chlorite (3) | | | | | | | | |
| Min | 32.86 | 0 | 6.97 | 0.64 | 6.64 | - | 0 | 28.31 | 0.27 | 0 | 0 | 0 | 0 | 84.44 |
| Max | 34.38 | 0 | 15.17 | 4.90 | 9.16 | - | 0 | 31.77 | 0.99 | 0 | 0 | 0 | 0 | 86.91 |
| | | | | | | titanite (2) | | | | | | | | |
| | 32.08 | 38.60 | 0.74 | 0 | 0 | - | 0 | 27.49 | 0 | 0 | 0 | 0 | 0 | 98.91 |
| | 32.41 | 39.45 | 0.59 | 0 | 0.58 | - | 0 | 27.76 | 0 | 0 | 0 | 0 | 0 | 100.79 |
| | | | | | | chromite (7) | | | | | | | | |
| Min | 0 | 0 | 12.17 | 39.07 | 12.49 | 1.40 | 0 | 2.28 | 0 | 0 | 0 | 0 | 0 | 98.56 |
| Max | 0 | 0.42 | 28.40 | 58.75 | 29.56 | 7.09 | 1.08 | 15.55 | 0 | 0 | 3.21 | 0.34 | 0.32 | 101.39 |
| | | | | | | ilmenite (1) | | | | | | | | |
| | 0 | 51.28 | 0 | 0 | 43.30 | - | 3.67 | 0 | 0 | 0 | 0 | 0 | 0 | 98.24 |

Notes: In brackets - the number of analyzes.

Local light green rodingite with a yellowish shade is traditionally called “californite”, that is, Californian jade. But as a result of the sample analysis, it turned out that it consists of hydrogrossular (Table 2), that is, it should be attributed to the Transvaal jade. There are minor amounts of vesuvianite and chlorite, forming veinlets and cloud-like aggregates.

**Table 2.** Chemical composition of rodingite minerals, wt. %.

| | $SiO_2$ | $Al_2O_3$ | FeO | MgO | CaO | ∑ |
|---|---|---|---|---|---|---|
| | | | grossular (5) | | | |
| Min | 34.00 | 19.78 | 0 | 36.17 | 0 | 90.69 |
| Max | 37.40 | 22.20 | 0.74 | 38.13 | 0 | 97.68 |

| | | | | | | |
|---|---|---|---|---|---|---|
| | | | chlorite (5) | | | |
| Min | 24.62 | 18.31 | 2.97 | 21.23 | 0 | 83.17 |
| Max | 31.13 | 25.32 | 16.52 | 31.54 | 0 | 84.46 |
| | | | vesuvianite (4) | | | |
| Min | 34.06 | 16.16 | 2.80 | 2.16 | 34.24 | 91.14 |
| Max | 36.24 | 16.67 | 3.04 | 2.65 | 36.28 | 94.13 |

Notes: In brackets - the number of analyzes.

Chemical analysis of another sample (Table 3) indicates that Californian jade, that is, vesuvianite, is also present at the deposit.

**Table 3.** Chemical composition of the rocks of the Nyrdvomenshor deposit, main components in wt. %. trace elements in ppm.

| | nephrite | | | diopsidite | rodingite |
|---|---|---|---|---|---|
| $SiO_2$ | 58.17 | 58.44 | 56.35 | 52.83 | 33.70 |
| $TiO_2$ | 0.03 | 0.03 | 0.04 | 0.08 | 0.05 |
| $Al2O_3$ | 0.33 | 0.28 | 0.66 | 0.40 | 19.48 |
| $Fe_2O_{3\Sigma}$ | 5.07 | 4.87 | 5.88 | 8.13 | 5.19 |
| MnO | 0.10 | 0.11 | 0.11 | 0.11 | 0.04 |
| MgO | 21.70 | 21.68 | 21.49 | 16.42 | 10.91 |
| CaO | 12.57 | 12.06 | 13.04 | 21.40 | 28.80 |
| $Na_2O$ | 0.15 | 0.48 | 0.27 | 0.08 | 0.07 |
| $K_2O$ | 0.06 | 0.19 | 0.11 | 0.04 | 0.03 |
| $P_2O_5$ | 0 | 0.02 | 0.03 | 0.09 | 0 |
| S | 0.03 | 0.03 | 0.03 | 0.04 | 0 |
| Cr | 0.02 | 0.03 | 0.08 | 0.01 | 0.01 |
| LOI | 1.87 | 2.03 | 2.36 | 0.57 | 1.78 |
| $\sum$ | 100.09 | 100.26 | 100.42 | 100.20 | 100.08 |
| Li | 0.5 | 0.5 | 1.5 | 1 | 14 |
| Be | 0.11 | 0.2 | 0.23 | 0.25 | 0.013 |
| Sc | 2.8 | 3.7 | 6 | 5 | 12 |
| Ti | 40 | 40 | 60 | 210 | 110 |
| V | 15 | 15 | 16 | 21 | 26 |
| Cr | 400 | 440 | 700 | 380 | 70 |
| Mn | 340 | 400 | 380 | 380 | 170 |
| Co | 21 | 24 | 24 | 18 | 14 |
| Ni | 400 | 400 | 400 | 200 | 60 |
| Cu | 4 | 4 | 9 | 11.5 | 4 |
| Zn | 14 | 15 | 20 | 9 | 6 |
| Ga | 0.4 | 0.4 | 0.8 | 0.5 | 3 |
| Ge | 0.44 | 0.39 | 0.27 | 0.6 | 0.34 |
| As | < 0.02 | < 0.02 | < 0.02 | < 0.02 | < 0.02 |
| Se | 0.17 | 0.2 | 0.24 | 0.35 | 0.45 |
| Rb | 0.5 | 0.21 | 0.19 | 0.27 | 0.33 |
| Sr | 33 | 29 | 50 | 40 | 27 |
| Y | 0.17 | 0.3 | 0.6 | 2 | 0.8 |
| Zr | 0.19 | 0.16 | 0.4 | 6 | 0.8 |
| Nb | 0.26 | 0.19 | 0.16 | 0.4 | 0.08 |
| Mo | 0.29 | 0.28 | 0.28 | 0.6 | 0.29 |
| Ag | 0.0117 | 0.0111 | 0.0072 | 0.019 | 0.008 |
| Cd | 0.025 | 0.03 | 0.07 | 0.03 | 0.04 |
| Sn | 0.24 | 0.16 | 0.2 | 0.32 | 0.21 |

| | | | | | |
|---|---|---|---|---|---|
| Sb | 0.07 | 0.07 | 0.08 | 0.4 | 0.09 |
| Te | < 0.01 | 0.019 | < 0.01 | 0.017 | < 0.01 |
| Cs | 0.04 | 0.012 | 0.027 | 0.02 | 0.08 |
| Ba | 5.4 | 4.8 | 4.9 | 5.1 | 4.7 |
| La | 0.05 | 0.07 | 0.13 | 1.2 | 0.09 |
| Ce | 0.14 | 0.16 | 0.24 | 2.3 | 0.18 |
| Pr | 0.019 | 0.024 | 0.033 | 0.31 | 0.027 |
| Nd | 0.078 | 0.11 | 0.16 | 1.2 | 0.13 |
| Sm | 0.022 | 0.036 | 0.044 | 0.3 | 0.049 |
| Eu | 0.043 | 0.02 | 0.019 | 0.09 | 0.049 |
| Gd | 0.027 | 0.046 | 0.063 | 0.38 | 0.087 |
| Tb | 0.005 | 0.007 | 0.013 | 0.06 | 0.019 |
| Dy | 0.028 | 0.038 | 0.08 | 0.38 | 0.15 |
| Ho | 0.006 | 0.007 | 0.018 | 0.08 | 0.035 |
| Er | 0.017 | 0.021 | 0.059 | 0.24 | 0.11 |
| Tm | 0.0028 | 0.0031 | 0.009 | 0.035 | 0.016 |
| Yb | 0.019 | 0.026 | 0.07 | 0.22 | 0.12 |
| Lu | 0.003 | 0.005 | 0.01 | 0.04 | 0.019 |
| Hf | 0.1 | 0.024 | 0.023 | 0.21 | 0.04 |
| Ta | 0.13 | 0.05 | 0.037 | 0.11 | 0.045 |
| W | 0.3 | 0.26 | 0.4 | 0.8 | 3 |
| Tl | 0.004 | 0.003 | 0.005 | 0.0025 | 0.0027 |
| Pb | 0.19 | 0.3 | 0.6 | 0.8 | 0.6 |
| Bi | 0.0142 | 0.0051 | 0.0033 | 0.019 | 0.0039 |
| Th | 0.08 | 0.018 | 0.011 | 0.3 | 0.018 |
| U | 0.014 | 0.013 | 0.031 | 0.16 | 0.011 |

### *3.2. Characteristics of nephrite*

Nephrite is mostly heterogeneously colored; homogeneous color is less common (Figure 6). It is trickle-like grayish-green to olive-green; dark grayish-green, often with spots, flakes of lighter grayish-green color up to 3 mm across. Thin rare grains of ore minerals are characteristic. Ore mineral grains up to 2 mm in size, making up to 3% of the sample area, are evenly distributed in dark differences. In sample 2/21, there are numerous visually distinguishable needle-like tremolite crystals all over the surface. One can see matte weathering crusts of a lighter grayish-green color up to 0.5 cm thick. Translucency is up to 0.2 cm in dark differences, up to 0.5 cm in light ones.

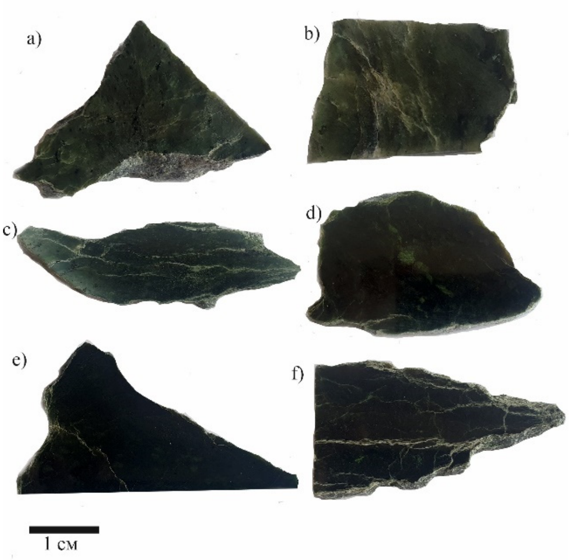

**Figure 6.** Nephrite samples: a) – 558; b) – 61-2; c) – 2/21; d) – 1/21; e) – 510-1; f) – 557-1.

Intense fracturing is observed, in the sample 2/21 it reaches foliation. Nephrite badly takes a polish, with intense shagreen and notches. Mirror polish is less often, but with cracks, or shagreen, an undulated pattern and cracks. Polishing is often heterogeneous: areas of extraneous mineral formation practically do not take a polish, they stay matte.

### *3.3. Mineral composition of nephrite*

We have studied the mineral composition of the nephrite. It is dominated by tremolite (Table 4) diverse in morphology from fine-fibrous to needle-like. Diopside (Table 4) forms relict grains (Figure 7e). Omphacite (Table 4, Figure 7a) overgrows grains of chromite and uvarovite (Table 4).

**Table 4.** Chemical composition of nephrite minerals, wt. %.

| | $SiO_2$ | $TiO_2$ | $Al_2O_3$ | $Cr_2O_3$ | FeO | $Fe_2O_3$ | MnO | MgO | CaO | $Na_2O$ | $K_2O$ | CoO | NiO | ZnO | $V_2O_3$ | Cl | F | ∑ |
|---|---|---|---|---|---|---|---|---|---|---|---|---|---|---|---|---|---|---|
| tremolite (35) | | | | | | | | | | | | | | | | | | |
| Min | 56.65 | 0 | 0 | 0 | 2.98 | - | 0 | 20.18 | 11.75 | 0 | 0 | 0 | 0 | 0 | 0 | 0 | 0 | 95.09 |
| Max | 59.99 | 0.35 | 0.66 | 0 | 4.80 | - | 0.37 | 23.45 | 13.75 | 0.85 | 0.51 | 0 | 0 | 0 | 0 | 0.40 | 1.48 | 99.90 |
| uvarovite (24) | | | | | | | | | | | | | | | | | | |
| Min | 33.93 | 0 | 0.43 | 12.32 | 0 | 0.47 | 0 | 0 | 30.80 | 0 | 0 | 0 | 0 | 0 | 0 | 0 | 0 | 98.38 |
| Max | 37.87 | 2.53 | 9.31 | 22.01 | 3.33 | 14.48 | 1.28 | 2.72 | 34.73 | 0 | 0 | 0 | 0 | 0 | 1.26 | 0 | 0 | 101.90 |
| diopside (7) | | | | | | | | | | | | | | | | | | |
| Min | 53.98 | 0 | 0 | 0 | 0.98 | 0 | 0 | 14.33 | 21.97 | 0 | 0 | 0 | 0 | 0 | 0 | 0 | 0 | 98.26 |
| Max | 55.24 | 0.30 | 2.42 | 1.77 | 3.49 | 2.13 | 0.50 | 17.44 | 24.91 | 1.95 | 0 | 0 | 0 | 0 | 0 | 0 | 0 | 102.00 |
| omphacite (10) | | | | | | | | | | | | | | | | | | |
| Min | 52.28 | 0 | 0.76 | 2.59 | 0.61 | 0 | 0 | 5.99 | 12.20 | 3.38 | 0 | 0 | 0 | 0 | 0 | 0 | 0 | 98.08 |
| Max | 56.31 | 0 | 6.59 | 10.11 | 6.03 | 4.04 | 2.47 | 12.04 | 18.23 | 6.31 | 0 | 0 | 0 | 0 | 0 | 0 | 0 | 101.92 |
| chlorite (5) | | | | | | | | | | | | | | | | | | |
| Min | 31.75 | 0 | 9.07 | 2.40 | 6.73 | - | 0 | 29.12 | 0 | 0 | 0 | 0 | 0 | 0 | 0 | 0 | 0 | 84.14 |
| Max | 35.26 | 0 | 12.34 | 5.89 | 8.17 | - | 0 | 30.74 | 0.71 | 0.65 | 0 | 0 | 0 | 0 | 0 | 0 | 0 | 88.76 |
| “shuiskite” (6) | | | | | | | | | | | | | | | | | | |
| Min | 11.96 | 0 | 1.59 | 24.44 | 13.05 | - | 0.99 | 0 | 11.05 | 0 | 0 | 0 | 0 | 0 | 0 | 0 | 0 | 97.79 |
| Max | 27.36 | 1.53 | 6.76 | 33.10 | 39.30 | - | 2.43 | 0.86 | 24.95 | 0.49 | 0 | 0 | 0 | 1.57 | 0 | 0 | 0 | 103.46 |
| chromite (23) | | | | | | | | | | | | | | | | | | |
| Min | 0 | 0 | 0 | 40.38 | 11.24 | 1.38 | 0 | 0.66 | 0 | 0 | 0 | 0 | 0 | 0 | 0 | 0 | 0 | 99.28 |
| Max | 0 | 1.83 | 38.60 | 58.54 | 27.92 | 22.95 | 3.49 | 17.68 | 0 | 0 | 0 | 0.64 | 0.43 | 1.79 | 0.43 | 0 | 0 | 101.98 |

Notes: In brackets - the number of analyzes.

Chlorite (Table 4) composes separate cloud-shaped isometric to elongated sections, cuts and overgrows chromite (Figure 7b, c), less often forms veinlets with grains of chromite and pentlandite. Chlorite, cutting or overgrowing chromite, contains more chromium and magnesium.

Chromite grains (Table 4) are rarely idiomorphic and homogeneous, more often they are fragmented, with an increased chromium and iron content (Figure 7b), or only iron (Figure 7c) to the periphery, cracks with chlorite and overgrows chromite. Chromite contains increased concentrations of manganese and zinc. Chromite is sometimes replaced by uvarovite along the periphery or in spots throughout the grain (Figure 7e).

Uvarovite forms mostly idiomorphic individual grains, sometimes sheath-like grains (Figure 7f), replaces chromite. Xenomorphic elongated grains are less often (Figure 7g). Uvarovite, forming independent grains, differs from the uvarovite, which replaces chromite by containing more Ti, Fe, especially trivalent (sometimes up to an intermediate composition between uvarovite and andradite), Mg and V, less Al, Mn and Cr.

Rare barite (BaO – 62.58 wt. %, SrO – 1.48 wt. %, $SO_3$ – 34,32 wt. %), millerite (Co – 3.50 wt. %, Ni – 60.69 wt. %, S – 37.13 wt. %), falcondoite, Fe-dominant mineral of the shuiskite group (Table 4, Figure 7h, i) are associated with chromite-uvarovite grains. Pentlandite (based on eight analyses, Fe – 22.19-24.78 wt. %, Co – 2.29-3.22 wt. %, Ni – 40.10-41.55 wt. %, S – 32.26-33.81 wt. %) forms xenomorphic elongated deformed and crushed grains.

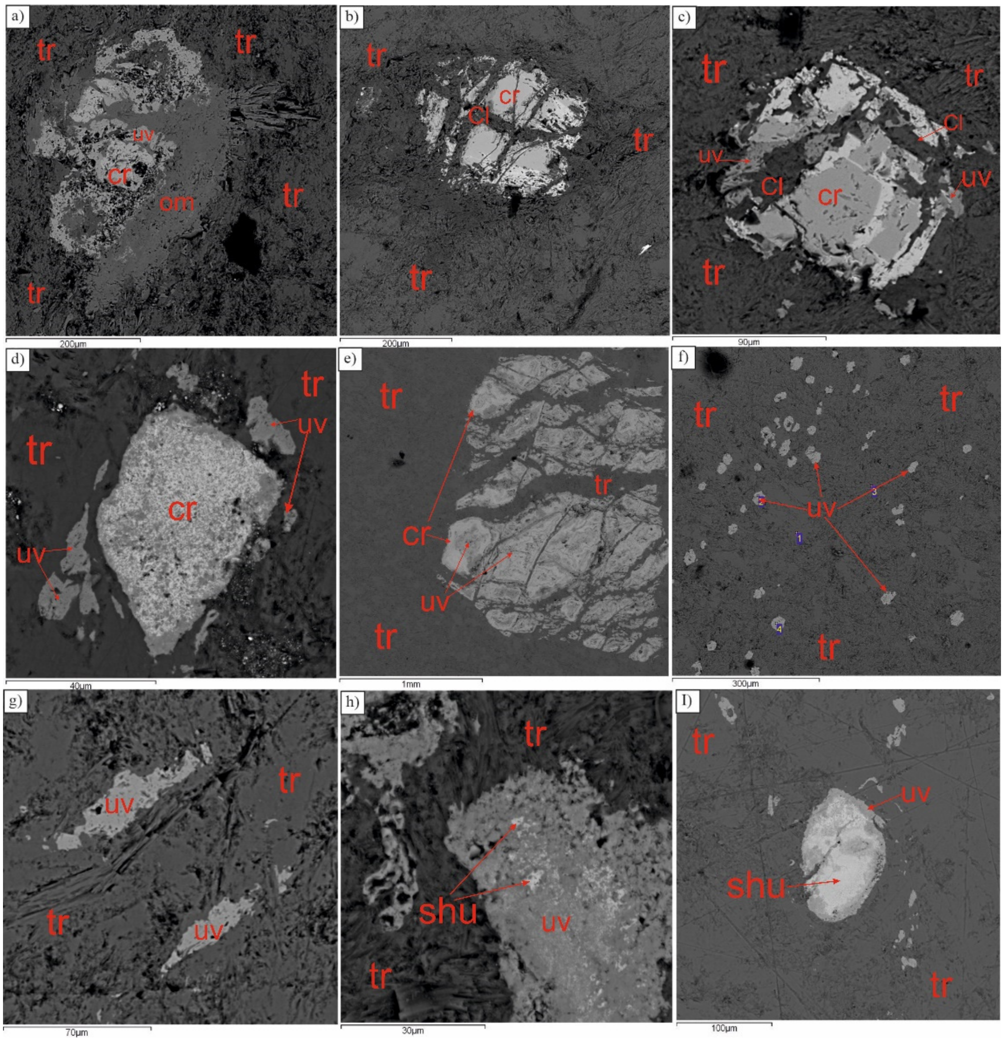

**Figure 7.** Mineral composition of nephrite: a) – in tremolite, chromite is corroded by uvarovite, and overgrows omphacite, 557-1; b) – chromite with chromium-ferruginous edges, stringers and chlorite overgrown in tremolite, 61-2; c) – chromite with ferruginous chromite edges is replaced by uvarovite, overgrown with chlorite, with tremolite around, 558; d) – chromite spots are replaced by uvarovite, individual grains of uvarovite among tremolite, 2-21; e) – uvarovite-chromite grain, where chromite is on the periphery, diopside grains in tremolite, 1-21; f) – sheath-like crystals of uvarovite in tremolite, 510-1; g) – elongated grains of uvarovite in tremolite, 557-1; h) - chromite-"shuiskite"-uvarovite (uvarovite is darker than "shuiskite") grain in tremolite, 1-21; i) – "shuiskite"-uvarovite grain in tremolite, uvarovite on the periphery, 510-1. Cl – chlorite, cr – chromite, dp - diopside, om - omphacite, tr – tremolite, shu – shuiskite, uv – uvarovite.

### *3.4. Isotope composition of the rocks*

We have studied the oxygen isotope composition of the rocks of the Nyrvomenshor deposit (Table 5). The isotope composition of diopsidites – 6.8 and 7.8 ‰ $\delta^{18}O$. The hydrogarnet rodingite values are even lower – 6.6 ‰ $\delta^{18}O$. Nephrites have a heavier isotope composition: 8.2-9.7 ‰ $\delta^{18}O$ (based on six analyses). The isotope composition of jadeite is close to nephrite – 8.8 % $\delta^{18}O$.

**Table 5.** Isotopic composition of Nyrdvomenshor deposit rocks.

| № | Sample | Rock | $\delta^{18}O$, ‰ VSMOW |
|---|---|---|---|
| 1 | 162 | diopsidite | 7.3 |
| 2 | 3/21 | diopsidite | 6.8 |
| 3 | | hydrogarnet rodingite | 6.1 |
| 4 | 558 | nephrite | 8.9 |

| | | | |
|---|---|---|---|
| 5 | 2/21 | nephrite | 8.6 |
| 6 | 510-1 | nephrite | 8.4 |
| 7 | 1/21 | nephrite | 8.2 |
| 8 | 61-2 | nephrite | 8.5 |
| 9 | 557-1 | nephrite | 9.7 |
| 10 | 66 | jadeite | 8.8 |

## 4. Discussion

Nephrite of the Nyrdvomenshor deposit is characterized by heterogeneous, unattractive coloration, jointing to foliation, low translucency. Therefore, in terms of its quality characteristics, it does not correspond to standard jewelry or ornamental nephrite.

The mineral composition of the Nyrdvomenshor nephrite is peculiar. Minerals such as omphacite, barite, millerite, falcondoite have not been previously observed in S-type nephrite. Fe-dominant shuiskite has not been described at all before.

Uvarovite is of even greater interest. It forms visually distinguishable secretions, is present in all samples in large quantities, forming independent grains and replacing chromite. Uvarovite was previously described in the nephrite of the Fentien deposit, Taiwan [12]. But the published garnet analysis results correspond to chromium grossular (11.6 wt. % $Cr_2O_3$ on average, maximum content is 12.86 wt. %, higher crystal core analysis results correspond to a mixture of chromium grossular and chromite). Uvarovite was mentioned as a mineral of nephrite of the Nyrdvomenshor and deposits of British Columbia, Canada without any analysis data attached [19].

Garnet of the grossular-uvarovite composition was found in the nephrite of the Nasławice deposit in Poland [26] and the Bazhenov chrysotile-asbestos deposit [36]. So far, the only reliable finding of abundant low-alumina uvarovite in S-type nephrite has been recorded at the Manas deposit in the Northern Tien Shan in the north of the Xinjiang Uygur Autonomous Region of China [7].

The S-type of nephrite was specified according to its chemical composition. It is believed that S-type nephrite has usual values of $Fe^{2+}/(Mg + Fe^{2+}) > 0.06$, whereas for D-type nephrite, it is $<0{,}06$ [46]. The Nyrdvomenshor nephrite value $Fe_2O_{3gen}/(MgO + Fe_2O_{3gen})$ varies within the range of 0.19-0.21 (Table 3). The content of Cr, Ni, Co in nephrite can also be used to distinguish S-type and D-type nephrite [46]. Cr (900-2812 ppm), Ni (958.7-1898 ppm) and Co (42-207 ppm) contents in S-type nephrite are relatively high, while Cr (2-179 ppm), Ni (0.05-471 ppm) and Co (0.5-10 ppm) contents in D-type nephrite are relatively low [46–49].

The content range is wider for Russian deposits. S-type nephrite on average: Ospa deposit – 1170 ppm of Cr, 1020 ppm of Cr, 65 ppm of Co (16 samples); Gorlykgol – 270, 1050, 97 (3); Bortogol – 580, 100, 53 (3); Ulankholda – 1200, 1400, 62 (26); Kitoy – 30, 120, 5 (1); Khamarkhuda – 660, 590, 54 (32); Param – 1500, 1250, 64 (8); Kelyana – 1700, 1800, 56 (1); Kurtushiba – 970, 1230, 61 (3); Agardak – 1100, 420, 42 (1); Khalilov – 180, 600, 22 (10); Kozmodemyanov – 800, 900, 50 (1). D-type nephrite of Russian deposits on average: 32, 19, 6 [19].

The content of these elements in Nyrdvomenshor nephrite (based on our data) is reduced (Cr 400-700 ppm, Ni 400 ppm, Co 21-24 ppm, Table 3), but it still corresponds to the S-type nephrite type. Previously, higher values are shown: 1110, 570, 68 based on 7 analyses [19]. Thus, the Nyrdvomenshor nephritie is typically S-type.

The content of rare earth elements (REE) ranges from 0.460 to 0.948 ppm (Table. 3), the distribution pattern is flat with a weak right slope – enrichment with light REE, positive Eu anomaly (Figure 8).

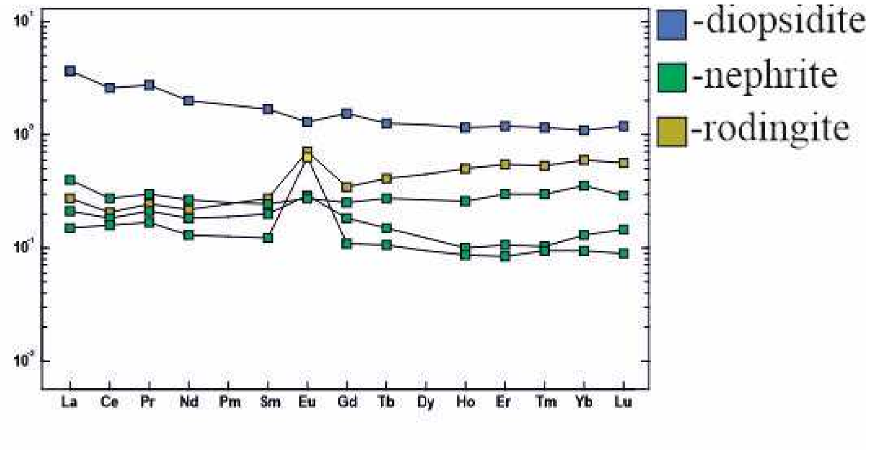

**Figure 8.** Normalized distribution of rare earth elements.

A positive Eu anomaly is observed at the Manas field, and a negative one – at the Eastern Sayan deposits with a right slope [7]. A positive Eu anomaly indicates a complex source of ore-forming fluid [7]. The Kutcho deposit has a left slope – enrichment with heavy REE, which is explained by the acidic environment of nephrite formation, and the weakly negative Eu anomaly is attributed to the reducing metallogenic environment [22]. The REE profiles of the Kutcho and Polar (Canada), Rim and South Westland (New Zealand), Golmud (Qinghai, China), Manas (Xinjiang, China) and Ulankhoda (Eastern Sayan, Russia) deposits are compared [22]. ΣREE contents ranged from 0.250 to 7.660 ppm – Kutcho nephrite has a higher ΣREE value (2.141–2.920 ppm), while a ΣREE value of New Zealand nephrite is the lowest (0.378–0.671 ppm). Since the value of ΣREE increases with decreasing pH, it is assumed that the metallogenic environment of Kutcho nephrite was very acidic. In relatively restorative conditions, δEu shows a negative anomaly, which is shown for all 5 deposits. Golmud, Manas and Ulankhod show the right slope [22]. Based on the peculiarities of the distribution of REE in the Nyrdvomenshor nephrites, it can be assumed that it was formed under the influence of a complex, non-acidic solution in an oxidizing environment.

The mineral composition reveals a complicated formation history of nephrite involving the combination of tectonic and metasomatic processes. At the progressive stage, serpentine is replaced by diopside:

$$Mg_3Si_2O_5(OH)_4 + 3Ca^{2+} + 4Si^{4+} + 5.5O_2 \rightarrow 3CaMgSi_2O_6 + 2H_2O.$$

Fluids containing calcium and silica come either from late intrusive bodies or as a result of long-range transport along tectonic ruptures.

At the regressive stage, the diopside is replaced by a tremolite aggregate - nephrite:

$$2CaMgSi_2O_6 + Mg^{2+} + 4Si^{4+} + H_2O + 5.5O_2 \rightarrow Ca_2Mg_5[Si_4O_{11}]_2(OH)_2.$$

This is indicated by relic grains of diopside. Relic chromite is crushed with an increase in the content of manganese and zinc, and replaced by uvarovite and “shuiskite”. Heazlewudite is replaced by pentladite – tremolite and pentlandite appear in a small amount in one sample of diopsidite. Chlorite and partially uvarovite of nephrite are inherited from diopsidite.

The third progressive stage led to the replacement of tremolite with omphacite (the reaction is not balanced due to the variable composition of the omphacite):

$$Ca_2Mg_5[Si_4O_{11}]_2(OH)_2 + Na^+ + Al^{3+} + Fe^{2+} + O \rightarrow (Ca, Na)(Mg, Al, Fe)Si_2O_6 + H_2O$$

and crushing of nephrite, which worsened its quality as an ornamental stone. Further process development with an increase in sodium and aluminum content should lead to the formation of jadeite $NaAlSi_2O_3$. Previously, the Nyrdvomenshor jadeite was believed [34] to be formed before nephrite.

An important indicator of nephrite formation processes is the isotopic composition of oxygen. At the Fengtien deposit in Taiwan, for the ordinary nephrite, $\delta^{18}O$ is 4.5-5.3 %, for the wax-like nephrite – 4.7-5.0 %, and for the nephrite with the “cat's eye” effect – 5.1-5.3%. Diopside from diopsidite – 3.7-4.5 %. It is concluded that nephrite inherits its composition from serpentinites and diopsidites [13]. The oxygen isotopic composition has been identified for a number of deposits of S-type nephrite in Russia: Param in Northern Transbaikalia, $\delta^{18}O$ – 6.13-9.54 ‰; Ospa in the Eastern Sayans – 8.43; Khamarkhudia in the Khamar-Daban – 6.72-7.87. It is believed that the fluid phase of nephrites transformed from serpentinites during metamorphism [50]. At the Jordanov deposit in Poland $\delta^{18}O$ is 6.1 %, for the shale nephrite – 6.7 [24]. The isotopic composition of oxygen at the S-type nephrite in the Chinese province of Qinghai is ($\delta^{18}O$) is 8.1, 8.6 ‰; in Russia – 8.2-8.5; in Canada – 9.4-12.3; in New Zealand – 4.7, 8.0; in Australia – 1.3, 1.6; in Pakistan – 13.0-13.4. It is shown that ore-forming fluids are formed as a result of metamorphism [51]. Single analyses were performed for the S-type nephrite from the Chara Dzhelgra River (?) in Siberia ($\delta^{18}O$ – 6.9), Red Mountain in New Zealand – 7.5, Mount Ogden, Canada – 9.6, the Shulaps Range, Canada – 8.4. These values are explained by the inheritance of the isotopic composition of the initial serpentinite with the possible influence of contacting metagabbro or crystalline shales [52].

At the Nyrdvomenshor deposit the isotope composition of diopsodites – 6.8 and 7.3 ‰ $\delta^{18}O$, and of hydrogarnet rodingite – 6.6 ‰ $\delta^{18}O$ indicates the deep origin of oxygen inherited from ultramafites that underwent serpentinization and metasomatosis – diopsidization with a small addition of the crustal component. Nephrites, apparently formed as a result of further metasomatism of diopsidites, have a heavier isotope composition: 8.2-9.7 $\delta^{18}O$. It indicates that crustal fluid contribution into metasomatism increases. Isotope composition of jadeite is close to nephrite – 8.8 % $\delta^{18}O$, since when nephrite is replaced with jadeite, it is not absorption, but disposal of the fluid.

Metamorphism reinforced metasomatic processes in the serpentinite melange, formation of a cryptocrystalline tangled-fibrous structure of nephrite, but then led to its fragmentation and replacement with omphacite. There are eight stages of the deformation process for the region [53], during which regressive and progressive regimes could replace each other.

The results obtained allow the subsurface user to refuse the license or adjust the territory of the subsurface site, and it allows the authorities of the Yamal-Nenets Autonomous Okrug to expand the natural park and make it more attractive due to additional knowledge. In case of criminal turnover, the specifics of the composition will allow to distinguish the Nyrdvomenshor nephrite, miming of which is currently not in the legal field.

## 6. Conclusions

Thus, the nephrite of the Nyrdvomenshor deposit is substandard. It was formed by both metamorphic and metasomatic processes. Initially, diopsidite formed after serpentinite, then it was replaced by nephrite. Metamorphism reinforced metasomatism in the serpentinite melange and provided the cryptocrystalline tangled-fibrous structure of the nephrite. Then, metamorphism and metasomatism resulted in omphacite formation and nephrite cracking, which reduced its quality. As these processes progressed, contribution of crustal fluid increased.

**Author Contributions:** Conceptualization, E.K., M.P. and F.N.; methodology, E.K.; software, V.V.; validation, E.K.; formal analysis, E.K.; investigation, E.K., M.P. and V.P.; resources, M.P. and F.N.; data curation, E.K. and M.P.; writing—original draft preparation, E.K.; writing—review and editing, E.K.; visualization, V.V.; supervision, E.K.; project administration, E.K.; funding acquisition, E.K. All authors have read and agreed to the published version of the manuscript.

**Funding:** This research was funded by Russian Science Foundation, grant number 22-27-20003, https://rscf.ru/project/22-27-20003.

**Data Availability Statement:** the data supporting reported results can provide by the corresponding author upon request.

**Acknowledgments:** The authors are grateful for the help in the work to technicians D.M. Vurms and A.V. Trofimov, analysts N.P. Gorbunova, L.A. Tatarinova, I.A. Zhelunitsyn, A.A. Nekrasova, D.V. Kiseleva and E.A. Khromova. Comments and suggestions of the editor and reviewers contributed to a significant improvement in the manuscript. The authors are grateful to the Federal State Budgetary Educational Institution of Higher Education "Ural State Mining University" for creating the conditions for performing work as part of the Federal program of strategic academic leadership "Priority 2030". The equipment of the Central Collective Use Centers "Geoanalyst" of the IGG UrB RAS, Yekaterinburg, and "Geospektr" of the GIN SB RAS, Ulan-Ude, was used.

**Conflicts of Interest:** The authors declare no conflict of interest.

## References

1. Kievlenko, E.Y. *Geology gems*. Ocean Pictures Ltd.: Littleton CO, USA. **2003**, 468 p.
2. Harlow, G.E.; Sorensen, S.S. Jade (Nephrite and Jadeitite) and Serpentinite: Metasomatic Connections. *Int. Geol. Rev.* **2005**, 47, 113–146.
3. Zhong, Q.; Liao, Z.; Qi, L.; Zhou, Zh. Black nephrite jade from Guangxi, Southern China. *Gems Gemol.* **2019**, 55, 198-215.
4. Zhang, Y.-D.; Yang, R.-D.; Gao, J.-B.; Chen, J.; Liu, Y.-N.; Zhou, Z.-R. Geochemical characteristics of nephrite from Luodian County, Guizhou Province, China. *Acta Mineral. Sinica* **2015**, 35, 56-64 (In Chinese with English abstract).
5. Flint, D.J.; Dubowski, E.A. Cowell jade province: detailed geological mapping and diamond drilling of jade and ornamental marble outcrops, 1982-1987. Department of mines and energy of South Australia. Rept. Bk. No. 89/51. Dme No. 85/88. **1991**. V. 2. 98 p. V. 3. 26 p. V. 4. 29 p.
6. Tan, T.L.; Ng, L.L.; Lim, L.C. Studies on Nephrite and Jadeite Jades by Fourier Transform Infrared (FTIR) and Raman Spectroscopic Techniques. *Cosmos* **2013**, 9, 47-56.
7. Wang, J.; Shi, G. Comparative Study on the Origin and Characteristics of Chinese (Manas) and Russian (East Sayan) Green Nephrites. *Minerals* **2021**, 11, 1434. https://doi.org/10.3390/min11121434
8. Yu, H.;Wang, R.; Guo, J.; Li, J.; Yang, X. Study of the minerogenetic mechanism and origin of Qinghai nephrite from Golmud, Qinghai, Northwest China. Sci. China Earth Sci. **2016**, 59, 1597–1609.
9. Zhang, C.; Yu, X.; Yang, F.; Santosh, M.; Huo, D. Petrology and geochronology of the Yushigou nephrite jade from the North Qilian Orogen, NWChina: Implications for subduction-related processes. *Lithos* **2021**. 380–381, 105894. doi.org/10.1016/j.lithos.2020.105894
10. Xu, Y.X.; Lu, B.Q.; Qi, L. J. A petromineralogical and SEM microstructural analysis of nephrite in Sichuan Province. *Shanghai Land and Resour.* **2015**, 36, 87–89. (in Chinese with English Abstract).
11. Zhang, C.; Yang, F.; Yu, X.; Liu, J.; Carranza, E.J.M.; Chi, J.; Zhang, P. Spatial-temporal distribution, metallogenic mechanisms and genetic types of nephrite jade deposits in China. *Front. Earth Sci.* **2023**, 11, 1047707. doi: 10.3389/feart.2023.1047707
12. Wan, H.M.; Yeh, C.L. Uvarovite and grossular from the Fengtien nephrite deposits, Eastern Taiwan. *Mineral. Mag.* **1984**, 48, 31-37.
13. Yui, T.-F.; Yeh, H.-W.; Lee, C.W. Stable isotope studies of nephrite deposits from Fengtien, Taiwan. *Geochim. Cosmochim. Acta* **1988**, 52, 593-602.
14. Yui, T.F.; Usuki T.; Chen, C.Y.; Ishida, A.; Sano, Y.; Suga, K.; Iizuka, Y; Chen, C.T. Dating thin zircon rims by NanoSIMS: The Fengtien nephrite (Taiwan) is the youngest jade on earth. *Int. Geol. Rev.* **2014**, 56, 1932–1944. doi:10.1080/00206814.2014.972994
15. Umar, Z.A.; Liaqat, U.; Ahmed, R.; Baig, M.A. Classification of Nephrite Using Calibration-Free Laser Induced Breakdown Spectroscopy (CF–LIBS) with Comparison to Laser Ablation–Time-of-Flight–Mass Spectrometry (LA–TOF–MS). *Anal. Letters* **2019**. doi:10.1080/00032719.2019.1643359
16. Obiadi, S.S.; Amini, M.A.; Fazli, F. Mineralogy and Geochemistry of Nephrite from Wolay Deposite, Kunar, East Afghanistan. *J. Mechanical, Civil and Industrial Engineering* **2022**. 3, P. 56-65.
17. Rehman, H.U.; Bilal; Owais, O.; Rahman, O.U; Shen A.H. Namak Mandi: a pioneering gemstone market in Pakistan. *Gems Gemol.* **2021**, 57, 138–149. dx.doi.org/10.5741/GEMS.57.2.138
18. Khan, R.A.; Anwar-ul-Haq M., Qasim M., Afgan M.S., Haq S.U., Hussain S.Z. Spectroscopic and crystallographic analysis of nephrite jade gemstone using laser induced breakdown spectroscopy, Raman spectroscopy, and X-ray diffraction. *Heliyon* **2022**, 8, e11493.
19. Suturin, A.N.; Zamaletdinov, R.S.; Sekerina, N.V. *Nephrite deposits*. ISU press: Irkutsk, Russia. **2015**. 377 p. (In Russian).
20. Boyd, W.F.; Wight, W. Gemstones of Canada. *J. Gemm*. **1983**, 18, 544-562.
21. Simandl, G.J.; Riveros, C.P.; Schiarizza, P. *Nephrite (Jade) Deposits, Mount Ogden Area, Central British Columbia (NTS 093N 13W).* British Columbia Geological Survey. Geological Fieldwork 1999, Paper 2000-1. **2000**. 339-347 pp.
22. Jiang, B.; Bai, F.; Zhao, J. Mineralogical and geochemical characteristics of green nephrite from Kutcho, northern British Columbia, Canada. *Lithos* 2021, 388–389, 106030. doi.org/10.1016/j.lithos.**2021**.106030.
23. Mills J. A Unique Occurrence of Nephrite Jade with Magnetite Inclusions in San Bernardino County, California. *Rocks Miner.* 2021, 96, 442-449. doi.org/10.1080/00357529.2021.1901208.
24. Gil, G.; Barnes, J.D.; Boschi, C.; Gunia, P.; Szakmany, G.; Bendo, Z.; Raczynski, P.; Peterdi, B. Origin of serpentinite-related nephrite from Jordanów and adjacent areas (SW Poland) and its comparison with selected nephrite occurrences. *Geol. Quarterly* **2015,** 59, 457-472.

25. Lobos, K.; Sachanbinski, M.; Pawlik, T. Nephrite from Naslawice in Lower Silesia (SW Poland). *Przeglad Geologiczny* **2008**, 56, 991-999. (In Polish with English abstract).
26. Gil, G.; Baginski, B.; Gunia, P.; Madej, S.; Sachanbinski, M.; Jokubauskas, P.; Belka, Z. Comparative Fe and Sr isotope study of nephrite deposits hosted in dolomitic marbles and serpentinites from the Sudetes, SW Poland: Implications for Fe-As-Au-bearing skarn formation and post-obduction evolution of the oceanic lithosphere. *Ore Geol. Rev*. **2020**, 118, 103335.
27. Adams, C.J.; Beck, R.J.; Campbell, H.J. Characterisation and origin of New Zealand nephrite jade using its strontium isotopic signature. *Lithos* **2007**, 97, 307-322.
28. Cooper, A.F. Origin and evolution of nephrites, diopsidites and giant diopside crystals from the contact zones of the Pounamu Ultramafics, Westland, New Zealand. *New Zealand J. Geol. Geophys*. **2023,** 66, 88-101. https://doi.org/10.1080/00288306.2022.2050771.
29. Tarling, M.S.; Smith, S.A.F.; Negrini, M.; Kuo, L.-W.; Wu, W.-H.; Cooper A.F. An evolutionary model and classification scheme for nephrite jade based on veining, fabric development, and the role of dissolution–precipitation. *Sci. Reports* **2022**, 12, 7823. doi.org/10.1038/s41598-022-11560-7.
30. Hockley, J.J. Nephrite (jade) Occurrence in the Great Serpentine Belt of New South Wales, Australia. *Nature* **1974**, 247, 364.
31. Coenraads, R.R. Gemstones of New South Wales. *Austral. Gemmologist* **1995**, 19, 91-107.
32. Krotov, B.P. Petrographic description of the southern part of the Miass dacha // *Society of Natural Scientists at Kazan University* **1915**, 47 (1), 402 p. (In Russian)
33. Mamurovskiy, A.A. *The nephrite deposit on Mount Bikilar*. Litogea: Moscow, Russia, **1918**. 52 p. (In Russian)
34. Kazak, A.P.; Dobretsov, N.L.; Moldavantsev, Y.E. Glaucophane shists, jadeites, vesuvianites and nephrites of the Rai-Iz hyperbasite massif. *Geol. Geophys.* **1976**, (2), 60-66. (In Russian)
35. Yushkin, N.P.; Ivanov, O.K.; Popov, V.A. *Introduction to topomineralogy of the Urals*. Nauka: Moscow, Russia, **1986**. 295 p. (In Russian)
36. Kislov, E.V.; Erokhin, Y.V.; Popov, M.P.; Nikolayev, A.G. Nephrite of Bazhenovskoye Chrysotile–Asbestos Deposit, Middle Urals: Localization, Mineral Composition, and Color. *Minerals*. **2021**, 11, 1227. doi.org/10.3390/min11111227
37. Knyazev, Y.G.; Knyazeva, O.Y.; Snachev, V.I.; Zhdanov, A.V.; Karimov, T.R.; Aidarov, E.M.; Masagutov, R.Kh.; Arslanova, E.R. *State Geological Map of the Russian Federation. Scale 1:1 000 000 (third generation). Ural Series. Sheet N-40 – Ufa. Explanatory note.* VSEGEI Map Factory: Sankt-Petersbourg, Russia. **2013**. 512 p. (In Russian)
38. Aerov, G.D.; Zaryanov, K.B.; Samsonov, Ya.P.; Gil'mutdinov, G.Kh. Colored stones in the hyperbasites of Kazakhstan. In *Geology, prospecting methods, exploration and evaluation of deposits of jewelry, ornamental and decorative facing stones*. All-Union 6th productions association under the Ministry of Geology of the USSR: Moscow, Russia. **1975**, pp. 16–18 (In Russian)
39. Arkhireev, I.E.; Maslennikov, V.V.; Makagonov, E.P.; Kabanova, L.Ya. South Ural nephrite province. *Razvedka i okhrana nedr* **2011** (3), 18–22 (In Russian)
40. Makagonov, E.P.; Arkhireev, I.E. Nephrite of the Urals. *Geoarchaeology and archaeological mineralogy* **2014** (1), 15-19. (In Russian)
41. Dobretsov, N.L.; Tatarinov, A.V. Jadeite and nephrite in ophiolites (the example of West Sayan). Nauka: Novosibirsk, Russia. **1983**. 126 p. (In Russian)
42. Gorbunova, N.P.; Tatarinova, L.A.; Kudyakova, V.S.; Popov, M.P. Wave X-ray fluorescence spectrometer XRF-1800 (SHIMADZU, Japan): method of determination of trace impurities in rubies. In: *Yearbook-2014. Proceedings of IGG UrB RAS*. **2015**, 162, pp. 238-241. (In Russian)
43. Sharp, Z.D. A laser-based microanalytical method for the *in situ* determination of oxygen isotope ratios of silicates and oxides. *Geochim. Cosmochim. Acta.* **1990**, 54, 1353-1357.
44. Vakhrusheva, N.V.; Shiryaev, P.B.; Stepanov, A.E.; Bogdanova, A.R. *Petrology and chromite content of the Rai-Iz ultrabasic massif (Polar Urals).* IGG UrB RAS: Ekaterinburg, Russia. **2017**. 265 p. (In Russian)
45. Sychev, S.N.; Kulikova, K.V. The sequence of deformations in the frame of the Rai-Iz massif (Polar Urals). *Vestnik of Saint Petersburg University. Series 7*. **2012,** (3), 53-59. (In Russian)
46. Siqin, B.; Qian, R.; Zhou, S.J.; Gan, F.X.; Dong, M.; Hua, Y.F. Glow discharge mass spectrometry studies on nephrite minerals formed by different metallogenic mechanisms and geological environments. *Int. J. Mass Spectrom*. **2012**, 309, 206–211.
47. Grapes, R.H.; Yun, S.T. Geochemistry of a New Zealand nephrite weathering rind. *N. Z. J. Geol. Geophys*. **2010**. 53, 413-426.
48. Liu, Y.; Deng, J.; Shi, G.; Yui, T.-F.; Zhang, G.; Maituohuti, A.; Yang, L.; Sun, X. Geochemistry and petrology of nephrite from Alamas, Xinjiang, NW China. *J. Asian Earth Sci.* **2011**. 42, 440-451.
49. Kostov, R.I.; Protochristov, C.; Stoyanov, C.; Csedreki, L.; Simon, A.; Szikszai, Z.; Uzonyi, I.; Gaydarska, B.; Chapman, J. Micro-PIXE geochemical fingerprinting of nephrite neolithic artifacts from Southwest Bulgaria. *Geoarchaeology*. **2012**. 27, 457-469.

50. Burtseva, M.V.; Ripp, G.S.; Posokhov, V.F.; Murzintseva, A.E. Nephrites of East Siberia: geochemical features and problems of genesis. *Russ. Geol. Geophys.* **2015**. 56, 402-410.
51. Liu, X.-F.; Zhang, H.-Q.; Liu, Y.; Zhang, J.; Li, Z-J.; Zhang, J.-H.; Zheng, F. Mineralogical characteristics and genesis of green nephrite from the world. *Rocks Mineral Anal.* **2018**. 37, 479-489. (In Chinese with English abstract). doi: 10.15898/j.cnki.11-2131/td.201712010187
52. Yui, T.-F.; Kwon, S.-T. Origin of a Dolomite-Related Jade Deposit at Chuncheon, Korea. *Econ. Geol.* **2002.** 97, 593–601.
53. Sychev S.N. Structure and evolution of the Main Ural Fault zone (southern part of the Polar Urals). Abstract of Kandidate (equal to PhD) Thesis. Geological Institute of Russian Science Academy, Moscow. 2015. 24 p. (In Russian)